

2017

Structural Transformations in Diluted Micellar and Lamellar Systems

Blanca Zelaya-Rincón
University of Rhode Island, blanca.zelaya.rincon@gmail.com

Follow this and additional works at: <https://digitalcommons.uri.edu/theses>

Recommended Citation

Zelaya-Rincón, Blanca, "Structural Transformations in Diluted Micellar and Lamellar Systems" (2017).
Open Access Master's Theses. Paper 1115.
<https://digitalcommons.uri.edu/theses/1115>

This Thesis is brought to you for free and open access by DigitalCommons@URI. It has been accepted for inclusion in Open Access Master's Theses by an authorized administrator of DigitalCommons@URI. For more information, please contact digitalcommons@etal.uri.edu.

STRUCTURAL TRANSFORMATIONS IN DILUTED
MICELLAR AND LAMELLAR SYSTEMS

BY

BLANCA ZELAYA-RINCÓN

A THESIS SUBMITTED IN PARTIAL FULFILLMENT OF THE
REQUIREMENTS FOR THE DEGREE OF
MASTER OF SCIENCE
IN
CHEMICAL ENGINEERING

UNIVERSITY OF RHODE ISLAND

2017

MASTER OF SCIENCE
OF
BLANCA ZELAYA-RINCÓN

APPROVED:

Thesis Committee:

Major Professor Arijit Bose

Geoffrey Bothun

Sze Cheng Yang

Nasser H. Zawia
DEAN OF THE GRADUATE SCHOOL

UNIVERSITY OF RHODE ISLAND
2017

ABSTRACT

The role of dilution by artificial hard water on nanostructures present in body wash samples provided by Procter and Gamble were investigated using time-resolved cryogenic transmission electron microscopy (cryo-TEM). Samples with and without perfume were examined at 10X, 20X, and 50X dilution. Micellar samples transformed to mostly unilamellar vesicles at 50X dilution, in contrast to the micelle to monomer transition seen in typical samples. At lower dilutions, a change in morphology from spherical to wormlike micelles was observed. For lamellar samples, lower dilution ratios show tightly packed multilamellar vesicles, while higher dilution ratios show more dispersed vesicles with less bilayers. Nanostructural transformations upon dilution were attributed to changes in curvature/packing parameters, which occurred due to dilution with hard water and addition of perfume. The systems experience changes in curvature in order to maintain equilibrium. Also, the addition of perfume in the lamellar samples caused an increase in the number of bilayers present in multilamellar vesicles, because of its role in increasing the packing parameter in the system.

ACKNOWLEDGMENTS

Words are not enough to express my gratitude to my Major Professor, Arijit Bose, who has helped, supported, and guided me throughout the whole process.

Thank you to Procter and Gamble for providing the samples and financial support for this study. Thank you to Richard Kingsley at URI for providing cryo-TEM sample preparation and operation training, as well as for taking the images used in this study. Also, thank you to Yanjing Chen at URI for training/help with role transition given at the beginning of this study.

Additional thank you to Rosi Smith, Rebekah Gomez, Maria Liebhauser, and their families for all of the love and support.

Thank you to my mother's side of the family for always being by my side. Without all of your love, support, help, encouragement, and faith in me, I would not have been able to close this chapter in my life. Special thanks to my grandparents, my aunt Claudia, and my uncle Joel.

Finally, thank you to my mother who has always motivated my brother and me to do our best in life. Her strength, determination, and caring personality have inspired me to never give up.

TABLE OF CONTENTS

ABSTRACT	ii
ACKNOWLEDGMENTS	iii
TABLE OF CONTENTS	iv
LIST OF TABLES	v
LIST OF FIGURES	vi
CHAPTER 1	1
INTRODUCTION	1
CHAPTER 2	3
EXPERIMENTAL METHODS.....	3
CHAPTER 3	7
RESULTS AND DISCUSSION.....	7
CHAPTER 4	15
CONCLUSION.....	15
APPENDIX	17
BIBLIOGRAPHY	30

LIST OF TABLES

TABLE	PAGE
Table 1. Chemical names and structures of surfactants and salt present in original samples received from Procter and Gamble	4

LIST OF FIGURES

FIGURE	PAGE
Figure 1. Blotless method schematic for cryo-TEM sample preparation.	5
Figure 2. Summary of Micellar sample, vortex mixed for 15 seconds, cryo-frozen within 20 seconds using blotless method: A,B,C) no perfume; D,E,F) with perfume; A,D) 10x dilution; B,E) 20x dilution; C,F) 50x dilution. Red arrows indicate micelles. Blue arrows indicate initial transition to small vesicles. Purple arrows indicate vesicles.....	7
Figure 3. Graph showing how the area of the vesicles present changes due to dilution for the micellar samples with and without perfume at 10x, 20x, and 50x dilution. The black squares and error bars indicate area values (in nm ²) for Mi samples at the different dilutions, and the red circles and error bars indicate area values (in nm ²) for MiP samples at the different dilutions.....	8
Figure 4. Graphs showing the areas of the vesicles present for each dilution in nm ² . The black bars indicate Mi samples and the red bars indicate MiP samples	9
Figure 5. Summary of Lamellar sample, vortex mixed for 15 seconds, cryo-frozen within 20 seconds using blotless method: A,B,C) no perfume; D,E,F) with perfume; A,D) 10x dilution; B,E) 20x dilution; C,F) 50x dilution. Purple arrows indicate unilamellar vesicles. Green arrows indicate multilamellar vesicles. Pink arrows indicate bilamellar vesicles. As dilution increases, curvature increases, causing transformations from larger vesicles to smaller vesicles with less layers.....	10
Figure 6. Graph showing how the area of the vesicles present changes due to dilution for	

the lamellar samples with and without perfume at 10x, 20x, and 50x dilution. The black squares and error bars indicate area values (in nm^2) for La samples at the different dilutions, and the red circles and error bars indicate area values (in nm^2) for LaP samples at the different dilutions.11

Figure 7. Graphs showing the areas of the vesicles present for each dilution in nm^2 . The black bars indicate La samples and the red bars indicate LaP samples.12

CHAPTER 1

INTRODUCTION

Body wash is an important consumer product. It consists of a complex mixture of surfactants and polymers, designed to produce rapid detergency action upon mixing with water and rubbing on skin, while providing the right feel for the user and being gentle on the skin [1, 2]. Its properties and performance are intimately related to the nanostructures present in the wash and changes to these nanostructures taking place because of dilution and mixing with water [1].

Micellar and lamellar systems can be found in many consumer products such as body wash, laundry detergent and shampoo [3]. These consumer product formulations often contain salts and perfume/raw materials, as well as different types of surfactants. There have been many studies focusing on the effects which the addition, removal, and change in concentration of these components have on these systems, as well as how shear affects the structures present in these systems [3-13]. Even so, there is still limited understanding as to how dilution affects the nanostructures present.

The skin barrier is a powerful film, made up of three major components: free fatty acids, ceramides, and cholesterol [14, 15]. A properly functioning skin barrier keeps out allergens, foreign materials, and reduces transepidermal water loss, therefore reducing skin dryness and irritation by keeping the balance between moisture and hydration, ultimately preventing skin diseases such as atopic dermatitis [15-17]. It is well known that certain surfactants such as SLS can be very harsh on the skin and actually strip the skin, meaning that although effective for cleansing all of the dirt and unwanted particles from skin, they also remove some of these major components of many of the skin barrier

[18]. This stripping of the skin barrier can cause slower skin regeneration after irritation occurs, and also makes penetration of foreign material and allergens easier, which can lead to conditions such as atopic dermatitis [16, 19]. Although there are now many gentler surfactants which are being studied and used, structural transformations in nanostructures present in these cleansing formulations can also have a drying effect, since it has been suggested that smaller nanostructures present in cleansing products tend to be more irritating to skin [19, 20].

This study focuses on the effects of dilution on the nanostructures present in micellar and lamellar systems. Specifically, the micellar and lamellar systems in this study are diluted with a salt solution (hard water), meaning that it may cause unexpected transformations to take place upon dilution [21]. However, there are many other factors which also need to be taken into consideration when diluting a system, such as mixing time, mixing method, whether or not perfume is present in the sample, and the sample preparation technique for cryogenic transmission electron microscopy (cryo-TEM).

Investigating what kinds of nanostructural transformations occur in different surfactant systems upon dilution with hard water, and using the results from this study in conjunction with previous knowledge regarding the maintenance of the skin barrier integrity, may be useful in the future optimization of body wash formulations, as well as cleansing formulations in general, to minimize skin irritation, dryness, and diseases such as atopic dermatitis.

CHAPTER 2

EXPERIMENTAL METHODS

Sample Preparation

Artificial hard water was made by adding 4.1 mg of calcium chloride dihydrate and 6.2 mg of magnesium chloride hexahydrate to 50 mL of DI water [22]. Total permanent water hardness was calculated by first calculating the concentration of Ca^{2+} and Mg^{2+} present in the DI water (in mg/L), since these are the prime cation contributors to water hardness [23]. These values were then expressed as equivalents of CaCO_3 and were added together to obtain a total hardness value [23]. The hard water used throughout this study was calculated to have a total hardness of 117 mg/L which is classified as moderately hard [24]. This method for making hard water in a laboratory is considered to be standard and was used because it most closely imitates the water people have access to in their homes [25].

The body wash samples were provided by Procter and Gamble. Samples of 10X dilution were made by mixing 300 microliters of original sample with 2700 microliters of hard water. Samples at 20X dilution were made by mixing 150 microliters of original sample with 2850 microliters of hard water, and samples at 50X dilution were made by mixing 60 microliters of original sample with 2940 microliters of hard water.

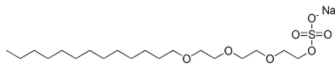
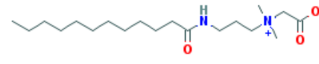
Sample Mixing

When body wash is used in the shower, a substantial amount of foam is produced with ease via dilution and scrubbing action. In order to mimic this production of foam samples were vortex mixed for 15 seconds, and then vitrified within 20 seconds after mixing. This mixing time of 15 seconds was chosen through personal experience and

inquiry about how long (on average) acquaintances spent using body wash while showering. Only the liquid layer was imaged.

The four original samples received from Procter and Gamble were: micellar no perfume (Mi), micellar with perfume (MiP), lamellar no perfume (La) and lamellar with perfume (LaP). Dilution will be indicated after these labels in order to indicate samples being referred to throughout this study (e.g. Mi10x would refer to the micellar sample with no perfume at 10x dilution).

Table 1. Chemical names and structures of surfactants and salt present in original samples received from Procter and Gamble.

Chemical Name	Formula	Structure	Molecular Weight	Sample Presence
Sodium Trideceth-2 Sulfate	$C_{19}H_{39}NaO_7S$ [26]	 [26]	434.564	Mi, MiP, La, LaP
Cocamidopropyl Betaine	$C_{19}H_{38}N_2O_3$ [27]	 [27]	342.524	Mi, MiP, La, LaP
Trideceth-3	$C_{13}H_{27}(CH_2CH_2O)_3OH$	$C_{13}H_{27}$ → branched hydrocarbon; approximately 2-3 methyl branches at random positions	332.525	La, LaP
Sodium Chloride	NaCl	$Na^+ - Cl^-$	58.44	La, LaP

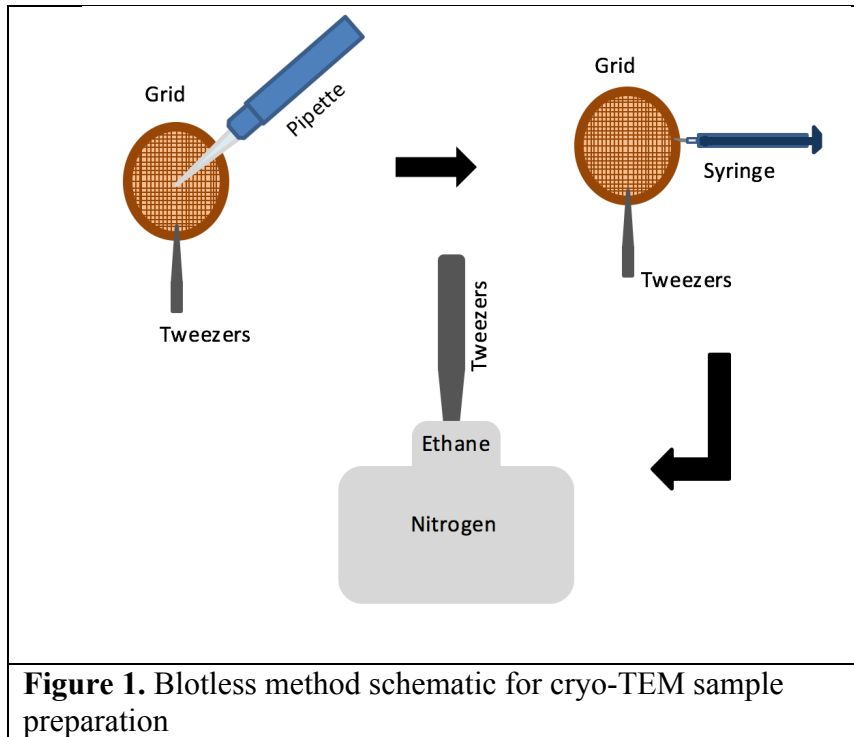
Note: Information for Trideceth-3 (formula and structure) given by Procter and Gamble

The table above shows the main/important components of the samples, which are mainly surfactants which were present. The chemical names were given by Procter and Gamble.

Cryogenic Transmission Electron Microscopy (cryo-TEM)

A blotless method was chosen for cryo-TEM sample preparation to avoid artifacts created by shear [28]. After pipetting the sample onto a holey carbon grid, excess liquid

was removed via syringe or capillary tube. The syringe (or capillary tube) was placed parallel to the plane of the grid as seen in the figure below.



This geometry allowed sample to be thinned out without introducing any flow within the grid holes, therefore removing any shear-induced artifacts from the sample and images [28]. The sample was then vitrified in ethane and stored in a liquid nitrogen dewar until it was imaged. The grid was placed on a Gatan 626 DH cryo holder, inserted into a JEOL 2100 TEM. The sample's temperature was maintained at -165C during imaging.

Image Analysis

In order to estimate vesicle size (area in nm^2) ImageJ was used. The diameter of the vesicles was measured directly when round vesicles were present. However, for irregularly shaped vesicles the diameter had to be estimated in order to calculate the area as accurately as possible. The particle analysis functions were tested, but were not used

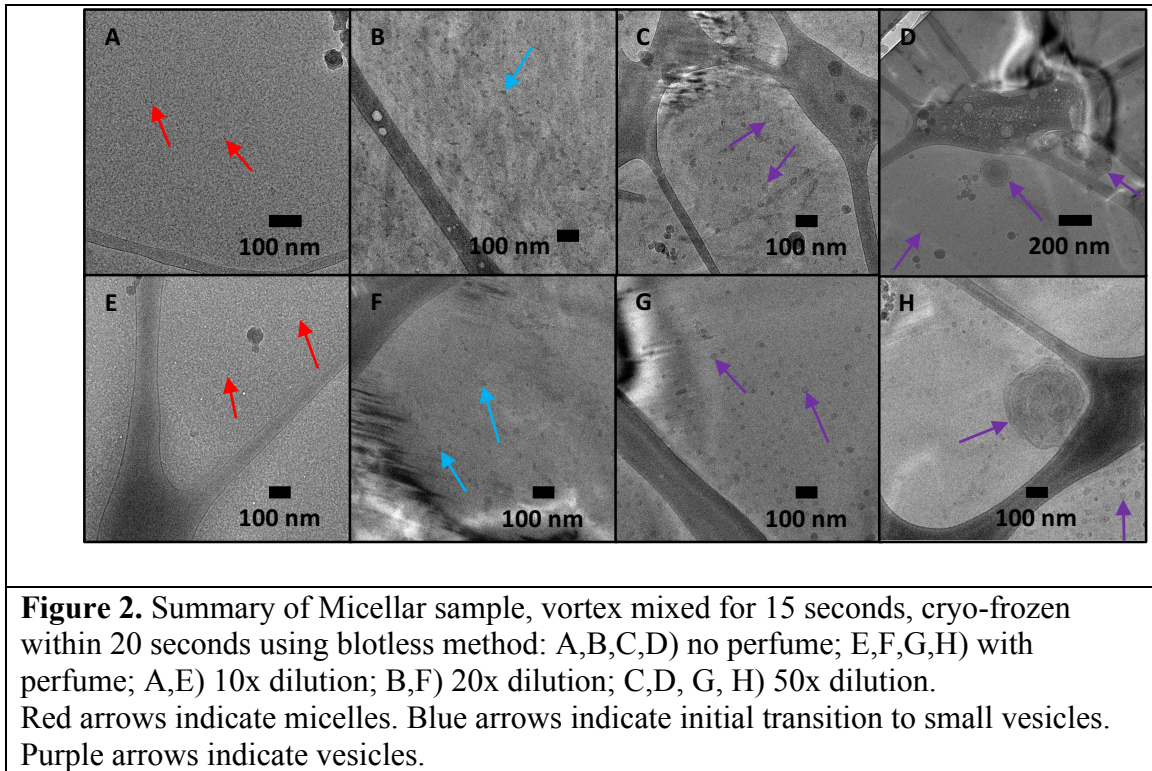
due to the complex nature of the systems imaged and low image contrast. Manual analysis proved to be the most effective choice for this study.

Results obtained through ImageJ analysis were averaged and the mean areas were plotted. Standard deviations are reported as error bars. They were also graphed as histograms. The outliers in the data were not included in the graphs, due to the fact their large values distorted the axis, making the smaller vesicle areas more difficult to visualize. However, they are included and highlighted in yellow in the Appendix.

CHAPTER 3

RESULTS AND DISCUSSION

Images of the micellar samples with and without perfume at the different dilutions are shown in Figure 2.



From these images, it can be seen that in general, as the dilution increases the size of the structures increases in the micellar system with no perfume. Also, when less dilute, there are no vesicles present in the system. Only micelles and wormlike micelles can be seen.

Figure 3 shows a graph indicating how the area of the vesicles present in the samples changes due to dilution.

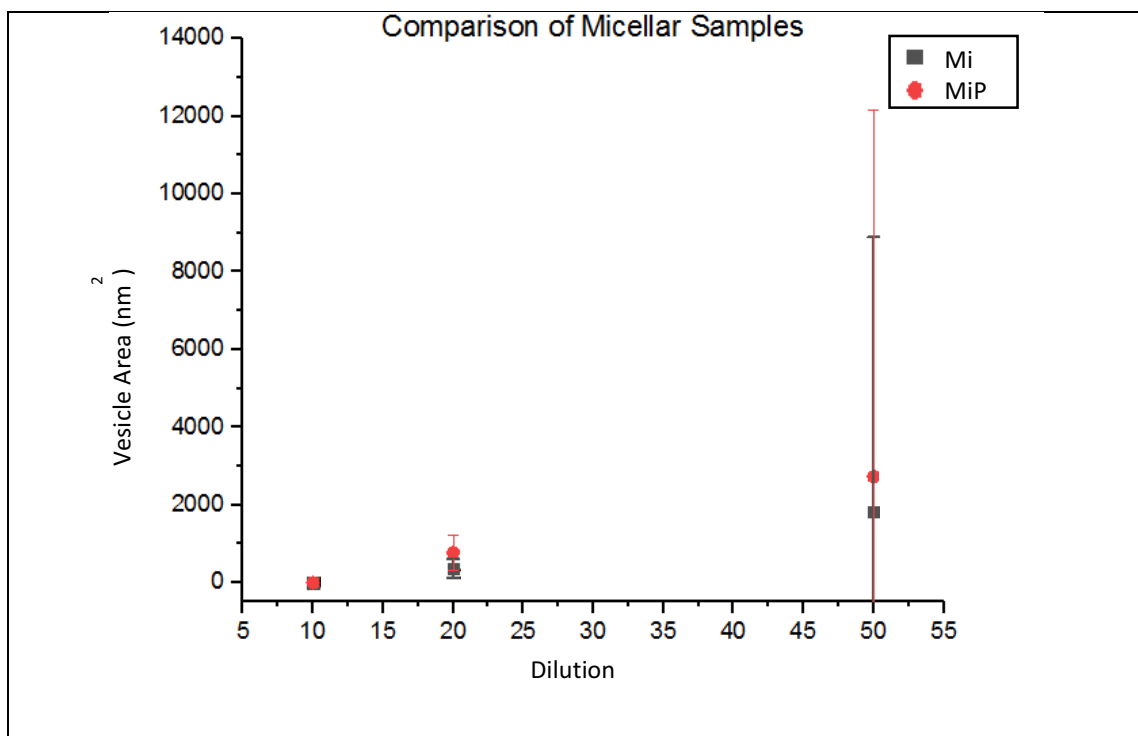
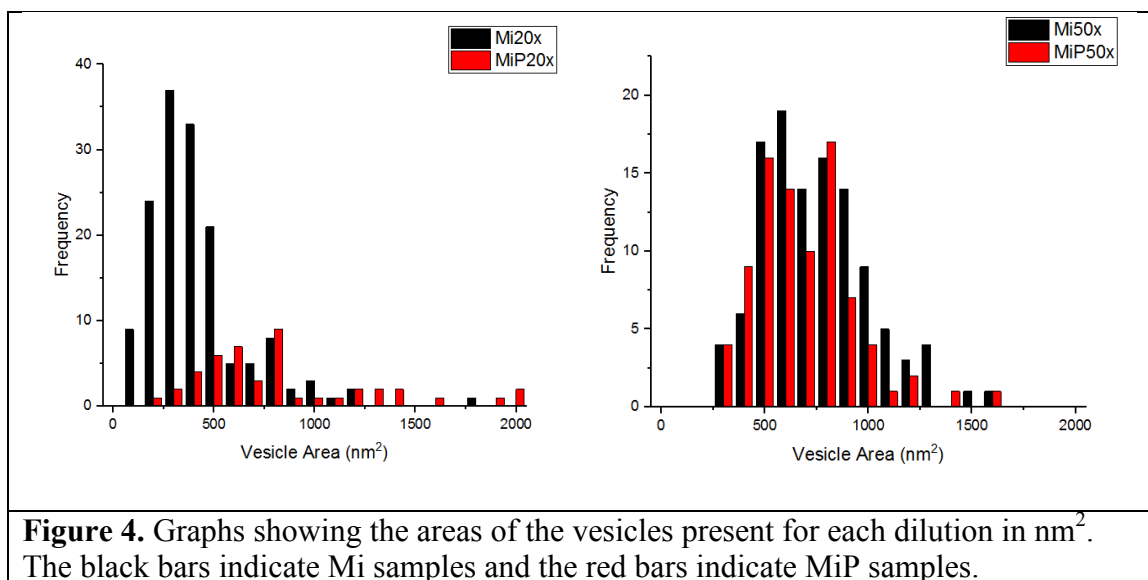


Figure 3. Graph showing how the area of the vesicles present changes due to dilution for the micellar samples with and without perfume at 10x, 20x, and 50x dilution. The black squares and error bars indicate area values (in nm²) for Mi samples at the different dilutions, and the red circles and error bars indicate area values (in nm²) for MiP samples at the different dilutions.

From this graph, the size increase due to dilution as seen in the Mi and MiP images from figure 2 can be confirmed. Figure 4 shows graphs of the micellar samples at 20 and 50 times dilution. When compared to figure 3 above, the overall size increase upon dilution can be confirmed, as well as the fact that there is more variability in the micellar samples at 50x dilution. It should be noted that for both the Mi and MiP samples at 50 times dilution, there are some larger values which were included in these graphs, which are highlighted in the appendix. These larger values also contribute to the large standard deviation seen figure 3.



This is different from what is usually expected, as micelles would usually transform into monomers upon dilution, since the surfactant concentration in the system would be below the CMC [29]. However, in this case the systems were diluted with hard water, which is a salt solution. The addition of salts to micellar systems have been shown to increase the packing parameter by reducing headgroup repulsion, even at low surfactant concentrations, therefore inducing micelle/wormlike micelle formation [3, 30, 31]. As more salt solution is added to the system, the packing parameter continues to increase, and eventually vesicle formation becomes more favorable, as seen in the vesicle images in figure 2 [21, 32]. Initially, salt is absent from the original micellar samples, as shown in table 1, which further suggests that the reason for vesicle formation is the addition of salt via hard water. However, as the dilution increases and the surfactant ratio decreases, the addition of salt would have less of an impact and the system would follow the logical transition from vesicles to micelles and eventually to monomers.

It is known that the addition of perfume may alter the curvature and packing constraints of a system, depending on whether it acts as a co-surfactant and/or co-solvent,

therefore causing changes in the structures present [33-35]. It is more commonly assumed that perfume acts as a co-surfactant, allowing the formation of vesicles with more bilayers [33-35]. However, in the micellar samples, the perfume does not seem to have much of an effect. The only noticeable effect is that the standard deviation for the samples with perfume is larger than the standard deviation for the no perfume samples, meaning that there is a larger size distribution in the perfume samples. Given the large standard deviation overall, there is not a noticeable difference in the sizes of the structures found in the Mi and MiP samples.

The remaining figures show images of the lamellar systems with and without perfume at 10x, 20x, and 50x dilution.

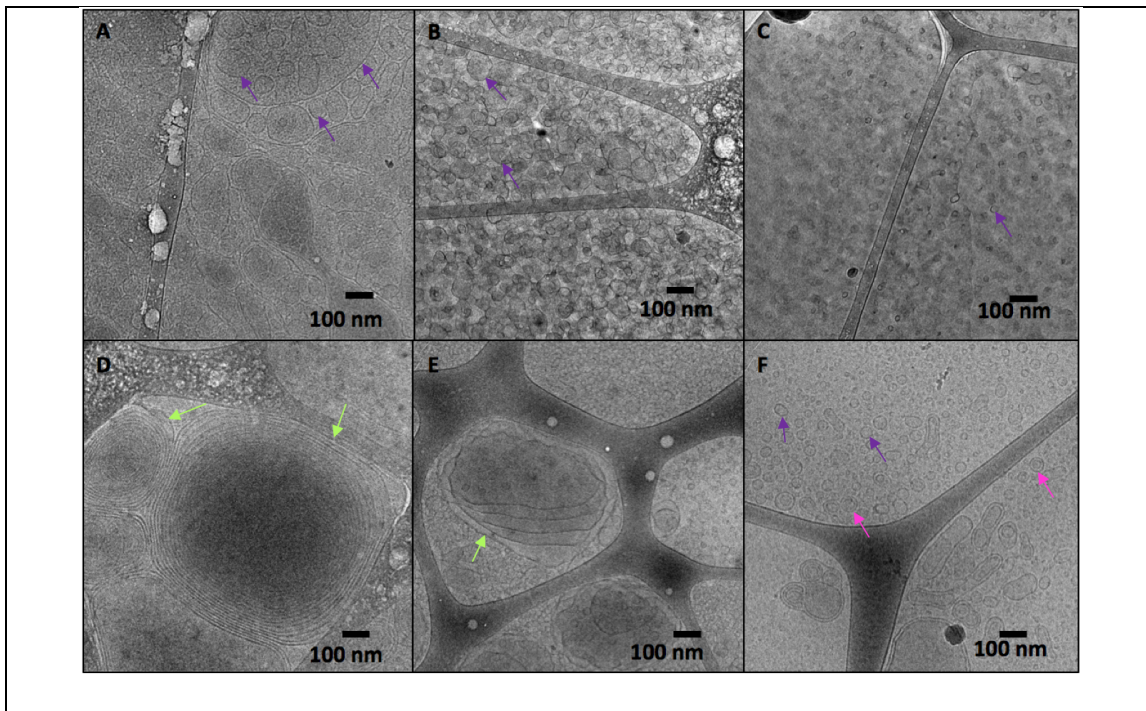


Figure 5. Summary of Lamellar sample, vortex mixed for 15 seconds, cryo-frozen within 20 seconds using blotless method: A,B,C) no perfume; D,E,F) with perfume; A,D) 10x dilution; B,E) 20x dilution; C,F) 50x dilution. Purple arrows indicate unilamellar vesicles. Green arrows indicate multilamellar vesicles. Pink arrows indicate bilamellar vesicles. As dilution increases, curvature increases, causing transformations from larger vesicles to smaller vesicles with less layers.

As a general trend, both lamellar systems (with and without perfume) show a decrease in vesicle size with increase in dilution ratio. This is quite different from the micellar samples which showed changes from wormlike micelles and micelles to vesicles. In lamellar systems, the addition of salt has less of an effect on the structural transformations, while the effects of perfume are more obvious. This can also be attributed to the fact that there was already some salt present in the original lamellar samples before the addition of hard water, as shown in Table 1. The only thing that salt may have an effect on is an increase in the lamellar repeat distance [36].

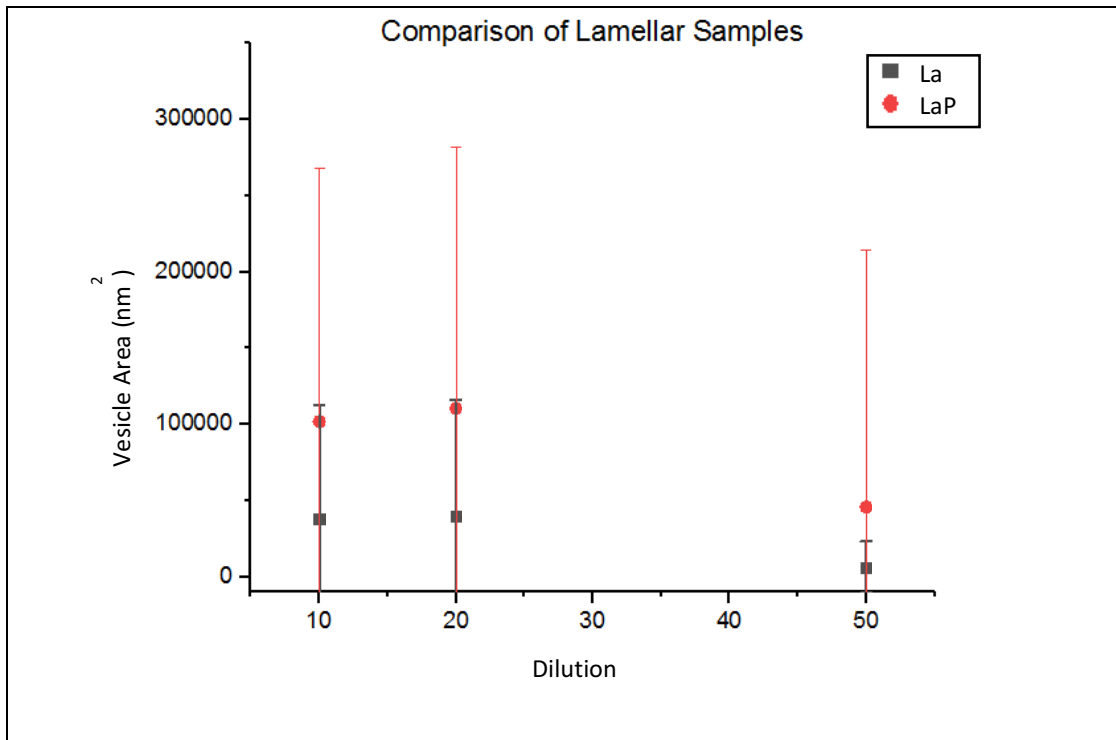
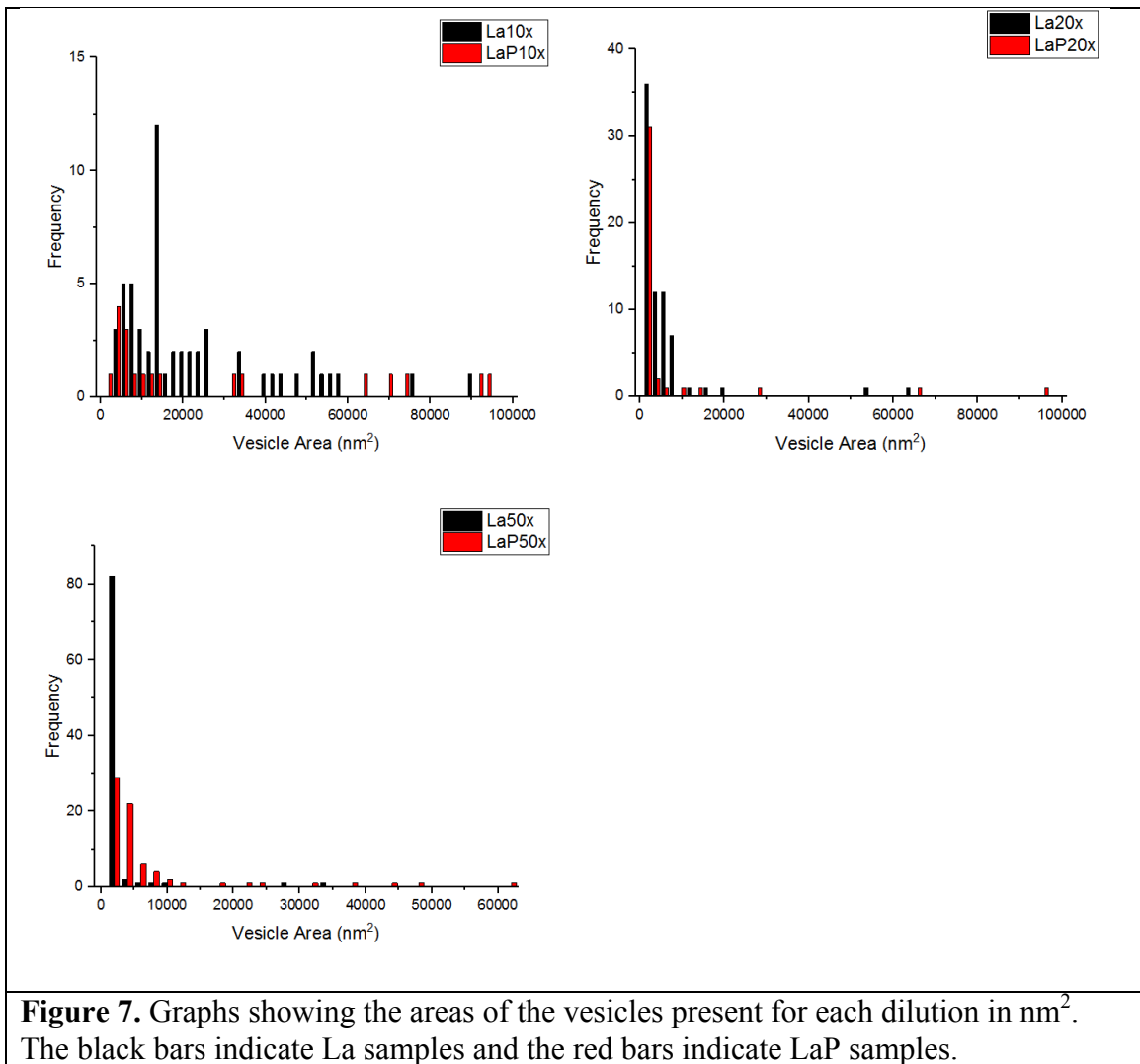


Figure 6. Graph showing how the area of the vesicles present changes due to dilution for the lamellar samples with and without perfume at 10x, 20x, and 50x dilution. The black squares and error bars indicate area values (in nm²) for La samples at the different dilutions, and the red circles and error bars indicate area values (in nm²) for LaP samples at the different dilutions.

Figure 6 shows a graph indicating how the area of the vesicles present in the samples changes as a function of dilution. However, like the micellar samples, the standard deviation is larger for the LaP samples, and smaller for the La samples, meaning that the size distribution is larger for the LaP samples. Given the large standard deviation, one might say that there is no change, however this is due to a smaller number of outliers present throughout the samples. Overall, it can be seen through the images that the area does decrease with an increase in dilution.



The general trend showing a decrease in size with dilution increase shown in the graph is in agreement with the visual results shown in figures 6 and 7. Another outcome that is initially surprising is that the average vesicle size at 20x dilution is slightly larger than the average vesicle size at 10 times dilution. However, upon closer inspection this makes sense for a few reasons. First, the variability for the samples at 20 times dilution are larger, meaning that the ranges of vesicle sizes are larger. Also, although the majority of the vesicles are smaller and have less bilayers at 20 times dilution, there are a few which are larger and contain many smaller vesicles within.

In aqueous solutions, surfactants often aggregate into structures, due to enthalpic or entropic driving forces [37, 38]. The curvature of this aggregate can change depending on many variables such as temperature, surfactant concentration, pH, as well as addition of electrolytes/salt, head group size, surfactant tail length, and number/types of surfactants present [39-41]. Structures formed in these systems depend on the curvature of these films, and in some instances these films form micelles by closing up [39]. Similarly, in systems with multiple surfactants present, surfactant bilayers may close up and form vesicles [39]. More specifically, the flexibility/rigidity of the film, which depends on the packing parameter, dictates what kind of aggregates are formed in the system; tail length and flexibility also have an effect on structures formed and on transitions that take place in mixed surfactant systems [30, 42-44].

Perfume seems to take on a co-surfactant role in the lamellar samples, due to the fact that the systems with perfume contain vesicles with many more layers than the ones found in the no perfume systems. By acting as a co-surfactant, the perfume would increase the surfactant efficiency by increasing the hydrophobicity of the surfactant, and

therefore increasing the packing parameter, causing vesicles to form more readily [34]. Although effects of shearing have been known to produce multilamellar vesicles in mixed surfactant systems, and are a factor in the structures present, the same shear was applied to the samples over the same timescale, therefore the increase in layer number from the no perfume sample to the sample with perfume can be directly attributed to the co-surfactant qualities of the perfume [45-49]. Also, since the amount of hard water added at each dilution is the same, salt cannot account for the difference in layers seen in the La and LaP samples.

Dilution expands the water layer, lowering the surfactant concentration present in the system. In order to maintain equilibrium, curvature must increase, causing the transition from larger vesicles to smaller unilamellar and bilamellar as seen in figure 5 [50, 51]. Therefore, a logical progression of expected structures observed with increasing dilution would be: multilamellar vesicles→unilamellar/bilamellar vesicles→micelles.

Since the micellar samples have a different formulation than the lamellar samples, the progression would be slightly different: wormlike micelle/micelle→unilamellar/bilamellar→ micelle, and eventually monomers. After dilution, the size of the structures would initially increase, and there would be a transition to vesicles, however upon further increase of the hydrophilic layer, the decrease in surfactant density would cause larger structures to break up and would transform into a more energetically stable micellar structure.

CHAPTER 4

CONCLUSION

As the dilution increases, initially micellar and lamellar systems seem to behave differently. Both micellar systems show an overall increase in the sizes of the nanostructures present, shown by the formation of larger, unilamellar vesicles from wormlike micelles/micelles. For lamellar samples, lower dilution ratios show tightly packed multilamellar vesicles, while higher dilution ratios show more dispersed vesicles with less bilayers. However, it has been predicted that both systems would eventually show transitions to from vesicles to micelles, and eventually monomers at even higher dilutions.

The effects of perfume on the nanostructures present in the samples were also considered, and it was found that the addition of perfume in lamellar samples caused more bilayers to form, though this did not always indicate a larger vesicles size. These effects indicated the role of perfume as a co-surfactant in the lamellar sample. In the micellar sample, the role of perfume was negligible. The mean area calculated for the samples with perfume was slightly larger than the no perfume sample, but due to the large standard deviation, it can't be said that perfume made a meaningful difference in the formulation.

Suggestions for future work

In order to see nanostructural transformations at smaller dilution increments, future experiments with more dilution ratios in between those used in this study (such as 15x, 30x, and 40x) should be tested. Also, in order to achieve a better understanding of what

the final nanostructures present are at higher dilutions, dilutions such as 120x, 150x, and 200x should be tested.

Some other suggestions for future work would be to use methods such as DLS in order to investigate the sizes of the nanostructures present more closely. The values obtained through DLS could then be compared to the values to the values obtained through cryo-TEM in this study.

APPENDIX

Mi 10x	Vesicle Area (nm ²)	MiP 10x	Vesicle Area (nm ²)
	0		0

Mi 20x	Vesicle Area (nm ²)	MiP 20x	Vesicle Area (nm ²)
	42.32532772		183.87789
	44.81710942		211.189171
	49.78909449		263.3670509
	62.23935184		300.6419543
	79.6748612		318.0353066
	89.61795482		360.2862681
	93.22756703		362.7801743
	99.57874818		422.4047888
	99.57874818		422.4047888
	102.0703453		459.6565245
	113.3802556		459.6565245
	123.7416044		482.0389679
	123.7416044		496.9400445
	143.5420081		509.3441833
	150.9617705		516.8117082
	160.8757322		526.7715779
	160.8757322		549.1341884
	161.8213296		576.4637668
	161.8213296		598.8052658
	161.8213296		598.8052658
	169.3013109		636.0608005
	171.3136871		648.5034402
	179.2447069		680.8077613
	179.2447069		715.6031469
	181.4106426		715.6031469
	181.745018		720.5427485
	181.745018		720.5427485
	184.2385881		720.5427485
	184.2385881		725.5470817
	186.4343988		740.4228214
	186.4343988		777.7287692
	199.1813921		787.6461489
	199.1813921		807.518294
	200.4591964		966.5711107
	201.5648988		1046.060052

	204.1398141		1195.14202
	210.3657219		1195.14202
	210.3657219		1217.488406
	211.6272826		1292.0692
	211.6272826		1316.907499
	211.6272826		1364.083948
	214.1617185		1552.909006
	222.7540624		1813.857619
	224.0787149		1900.779814
	224.0787149		1928.155871
	240.0611026		
	242.5390652		
	243.9765764		
	247.4773913		
	247.4773913		
	248.9574074		
	257.3895936		
	258.9274346		
	263.885065		
	271.36586		
	279.6621433		
	279.6621433		
	279.6621433		
	279.6621433		
	279.6621433		
	279.6621433		
	281.3244982		
	281.3244982		
	281.3244982		
	281.3244982		
	281.3244982		
	288.8058084		
	288.8058084		
	289.559339		
	289.559339		
	301.256921		
	301.256921		
	301.9341102		
	303.7230713		
	309.371014		

309.371014		
311.213108		
311.213108		
311.213108		
318.6678035		
321.7443267		
322.4759792		
323.6547292		
323.6547292		
338.5868518		
338.5868518		
338.5868518		
339.0762451		
339.0762451		
341.070086		
358.8746343		
358.8746343		
361.3299657		
363.4894713		
363.4894713		
366.2996629		
367.8277846		
367.8277846		
368.7461844		
368.7461844		
378.64819		
388.5765652		
390.8859751		
400.9369942		
403.3183882		
403.3183882		
405.8853584		
405.8853584		
405.8853584		
405.8853584		
408.1381372		
413.2026618		
420.7307472		
423.2430561		
428.1433971		

	428.2901095		
	430.7144922		
	445.479296		
	447.9517828		
	448.1393712		
	457.8722263		
	480.1340231		
	494.9664174		
	499.9474786		
	524.6989161		
	539.5403425		
	556.845043		
	574.1680323		
	577.5707541		
	606.3322712		
	614.7409827		
	618.746588		
	659.7456798		
	689.6231174		
	717.7383893		
	717.7383893		
	726.9800721		
	732.5822426		
	754.8650275		
	761.8448775		
	770.9224113		
	784.5650413		
	834.0241814		
	890.9633428		
	915.7344514		
	949.8371151		
	975.1312714		
	1051.858012		
	1133.518124		
	1133.518124		
	1725.802018		

Mi 50x	Vesicle Area (nm ²)	MiP 50x	Vesicle Area (nm ²)
	222.595368		226.4196413
	281.5921218		226.4196413

289.3784021	254.4124594
289.3784021	280.7599328
354.2892796	323.0173
365.0455901	325.6347525
378.4067986	337.9022948
378.4067986	348.541135
391.5871472	370.2111853
396.230641	370.2111853
426.7874991	379.0621828
429.5749148	390.080404
429.5749148	397.5371375
431.8187463	407.49385
431.8187463	419.8949728
436.2869213	429.9423555
436.2869213	432.4819774
439.9969851	442.2678374
439.9969851	442.2678374
442.8644385	447.2393049
445.1800656	457.910154
445.1800656	459.6565245
445.1800656	460.4548857
457.5688616	470.6274192
457.5688616	470.6274192
469.4361768	470.6274192
471.8971748	479.5516307
500.4628168	486.9938289
510.3847636	490.9916689
514.7989683	501.8912927
518.1826144	501.8912927
518.1826144	508.7843106
520.8489689	508.7843106
535.8823827	509.3441833
540.3228669	513.8744266
543.1281269	521.5368653
549.9652025	549.1341884
553.587425	559.0640056
556.4686762	559.0640056
563.1786155	562.2115869
571.961654	562.2115869
575.7405415	568.9982368

578.7214417	572.3856277
578.7214417	608.7350988
598.371616	608.7350988
598.371616	608.7350988
637.9844267	621.1738649
642.1547614	658.426075
642.1547614	661.4312314
642.3793577	680.8077613
642.3793577	684.327099
655.5638995	688.2739486
659.882266	697.0437611
663.3471663	714.8447162
663.3471663	715.6031469
673.1523377	718.070824
677.6204309	720.5427485
681.1315314	720.5427485
690.7872542	720.5427485
695.3133993	725.5470817
703.9867122	732.6781931
703.9867122	735.4634914
708.6030062	737.772562
712.2879813	757.8385175
712.2879813	757.8385175
717.4535065	777.7287692
721.2089923	777.7287692
726.3111673	796.2753633
726.3111673	796.2753633
748.4505991	796.2753633
752.8697369	805.0521681
752.8697369	807.518294
756.8141973	814.0793532
788.3427185	826.7713875
796.3753979	839.8184021
797.1759008	839.8184021
801.5858549	859.7103581
819.347314	906.905826
823.6146084	916.8611624
849.1928549	919.3316166
849.1928549	989.6307527
859.1907387	1075.849495

859.1907387		1124.465738
859.1907387		1144.764699
863.6645991		1383.991325
868.0456318		1562.843121
876.9984098		15509.47401
888.7426766		27562.78479
894.6175955		45181.64971
894.6175955		48501.27477
901.9485365		57058.48246
915.1445459		
943.7833045		
978.7876988		
978.7876988		
978.7876988		
978.7876988		
989.9653323		
996.5009375		
1007.553916		
1036.337294		
1073.583356		
1085.054707		
1085.054707		
1107.177453		
1151.491175		
1161.919904		
1210.879941		
1219.777761		
1244.477241		
1291.050017		
1439.328906		
1598.783145		
7783.29847		
29938.63035		
30750.33057		
64908.13204		

La 10x	Vesicle Area (nm ²)	LaP 10x	Vesicle Area (nm ²)
	2089.630009		1053.525733
	2594.013761		2149.277687
	3349.316181		2370.389752

4021.668495	2516.95929
4325.868017	3702.197021
4462.508966	4119.598545
4676.240436	4315.848234
5153.251822	4633.914622
6147.12604	6452.809448
7238.983476	8075.113946
7255.279501	10460.36065
7575.788397	12674.27104
7754.708842	30067.26877
8301.254	33538.51951
8525.933824	62514.27271
9504.00894	68222.36667
10080.46815	72743.41471
11792.80942	90645.21763
12339.87727	93841.65773
12584.83458	119887.0455
12584.83458	194128.4685
12587.41961	246902.0286
12951.13605	314160.7237
13191.0625	510115.3117
13337.22161	646879.4385
13390.08524	
13680.63101	
13698.0509	
13743.10359	
13906.909	
14808.78808	
16888.64416	
17223.8255	
18014.04449	
18393.31741	
20675.14602	
21529.93342	
23281.44249	
23736.09621	
24966.54615	
25760.85984	
25780.77744	
33027.292	

33710.45205		
38217.08737		
40731.13944		
43198.45064		
46131.86552		
50102.99954		
51226.0484		
53991.50597		
54625.12998		
57606.80638		
74343.54147		
88585.46777		
108629.282		
155405.4709		
364415.7015		
440871.5595		

La 20x	Vesicle Area (nm ²)	LaP 20x	Vesicle Area (nm ²)
	407.49385		248.4822046
	422.4047888		310.5880568
	459.6565245		318.0353066
	479.5516307		340.4157236
	503.8786642		360.2862681
	549.1341884		370.2111853
	568.9982368		422.4047888
	651.0787914		449.7166644
	718.070824		606.2449852
	720.5427485		606.2449852
	757.8385175		658.426075
	777.7287692		725.5470817
	777.7287692		735.4634914
	807.518294		757.8385175
	839.8184021		787.6461489
	906.905826		805.0521681
	940.4646761		807.518294
	970.3771023		827.3830744
	974.0246139		837.3546898
	977.8452375		974.0246139
	1046.060052		974.0246139
	1080.155915		978.9540626

1205.089213	1053.525733
1229.826742	1056.000993
1277.140371	1098.231077
1322.12265	1137.998133
1396.415595	1224.983198
1403.843677	1224.983198
1559.061627	1354.151727
1589.017878	1441.145072
1629.9754	1503.232451
1629.9754	2367.887862
1672.178792	2516.95929
1674.716543	4258.749103
1681.323701	9036.787149
1711.986839	12920.49417
2089.630009	27217.52461
2099.60775	64048.05115
2397.737348	94001.35767
2516.95929	161455.5257
2633.795263	216320.3589
2753.002795	216665.909
2818.863344	1043219.071
2886.168919	
2946.855155	
3508.41357	
3888.578953	
3968.00764	
4047.562743	
4238.877317	
4405.385663	
4810.3942	
4942.083091	
5014.115237	
5260.042854	
5399.271172	
5588.047064	
5588.047064	
5749.517937	
5916.014886	
6005.51025	
6087.515545	

	6124.772747 6298.688917 6348.584351 6899.968617 7195.616981 11292.96367 14111.6618 18371.68924 52627.13268 62758.69456 121678.9654		
--	--	--	--

La 50x	Vesicle Area (nm ²)	LaP 50x	Vesicle Area (nm ²)
	89.09855295		211.189171
	178.2021065		323.0173
	184.2385881		449.7166644
	210.3657219		541.6420844
	210.3657219		549.0926542
	220.2743468		613.2038289
	247.4773913		658.8354662
	263.885065		732.2944287
	309.371014		793.1274898
	321.7443267		793.1274898
	321.7443267		1013.582857
	323.6547292		1054.101116
	338.5868518		1097.174041
	360.9931241		1127.618041
	361.3299657		1228.956684
	363.4894713		1279.675322
	368.7461844		1279.675322
	400.9369942		1388.610895
	420.7307472		1391.121885
	420.7307472		1411.424638
	445.479296		1455.986145
	445.479296		1464.655935
	447.9517828		1552.909006
	447.9517828		1583.723215
	450.6192188		1621.756479
	460.5689938		1654.684705
	460.5689938		1707.882411

460.5689938	1745.888206
485.0791091	1890.361959
487.5415844	2108.225519
507.3460518	2141.150407
510.3847636	2153.881754
514.7587535	2283.101454
546.9350397	2308.23882
546.9350397	2354.022086
550.2146292	2354.022086
550.2146292	2447.375827
556.845043	2452.903099
560.1541666	2579.590081
562.631932	2627.704251
603.8470822	2648.643139
607.4675611	2725.63644
609.9601817	2882.170994
618.7024997	2894.649869
618.7024997	3167.420492
637.3578109	3180.40171
639.8212869	3259.8584
643.457967	3296.696966
655.8362191	3309.532298
659.7456798	3746.871451
677.1591195	3960.530573
677.1591195	4534.549905
689.6231174	5131.263216
715.2238813	5194.559267
726.9800721	5478.615889
732.5822426	5667.560934
736.9062364	5749.517937
774.6178078	6580.724994
774.6178078	6631.290085
774.6178078	6842.814706
784.5153955	6943.026959
784.5153955	8777.675917
806.6119319	9471.55145
809.1308609	10375.8745
816.609906	16580.02732
863.7166891	20641.51837
975.0759236	22351.92326

989.9653323	31908.55956
1120.309081	37839.30072
1125.297993	43342.24259
1244.789896	47321.10526
1274.671214	60532.45006
1294.618917	110106.9972
1356.827239	128041.7271
1366.769249	212890.657
1443.972496	
1458.895782	
1526.134315	
1645.61263	
1692.899296	
1843.797826	
1854.773696	
2519.449743	
2990.021333	
5599.182326	
6555.156254	
9923.591274	
26927.64037	
33181.76545	
241883.912	

BIBLIOGRAPHY

1. Bujak, T., T. Wasilewski, and Z. Nizioł-Łukaszewska, *Role of macromolecules in the safety of use of body wash cosmetics*. Colloids and Surfaces B: Biointerfaces, 2015. **135**: p. 497-503.
2. Regan, J., L.-M. Mollica, and K.P. Ananthapadmanabhan, *A Novel Glycinate-based Body Wash: Clinical Investigation Into Ultra-mildness, Effective Conditioning, and Improved Consumer Benefits*. The Journal of clinical and aesthetic dermatology, 2013. **6**(6): p. 23.
3. Tang, X., et al., *Multiscale Modeling of the Effects of Salt and Perfume Raw Materials on the Rheological Properties of Commercial Threadlike Micellar Solutions*. The Journal of Physical Chemistry B, 2017. **121**(11).
4. Mohanty, A., T. Patra, and J. Dey, *Salt-induced vesicle to micelle transition in aqueous solution of sodium N-(4-n-octyloxybenzoyl)-L-valinate*. The journal of physical chemistry. B, 2007. **111**(25): p. 7155.
5. Kusano, T., et al., *Structural and rheological studies on growth of salt-free wormlike micelles formed by star-type trimeric surfactants*. Langmuir : the ACS journal of surfaces and colloids, 2012. **28**(49): p. 16798.
6. Jiang, L., et al., *Bile salt-induced vesicle-to-micelle transition in catanionic surfactant systems: steric and electrostatic interactions*. Langmuir : the ACS journal of surfaces and colloids, 2008. **24**(9): p. 4600.
7. Uddin, M.H., N. Kanei, and H. Kunieda, *Solubilization and Emulsification of Perfume in Discontinuous Cubic Phase*. Langmuir, 2000. **16**(17): p. 6891-6897.
8. Mendes, E., et al., *A Small-Angle Neutron Scattering Study of a Shear-Induced Vesicle to Micelle Transition in Surfactant Mixtures*. The Journal of Physical Chemistry B, 1998. **102**(2): p. 338-343.
9. Wasilewski, T. and T. Bujak, *Effect of the Type of Nonionic Surfactant on the Manufacture and Properties of Hand Dishwashing Liquids in the Coacervate Form*. Industrial & Engineering Chemistry Research, 2014. **53**(34): p. 13356-13361.
10. Baruah, A., et al., *Phase Behavior and Thermodynamic and Rheological Properties of Single- (SDS) and Mixed-Surfactant (SDS + CAPB)-Based Fluids with 3-Methylbutan-1-ol as the Cosurfactant and Pine Oil as the Organic Phase*. Industrial & Engineering Chemistry Research, 2014. **53**(51): p. 19765-19774.

11. Oliver, R.C., et al., *Tuning micelle dimensions and properties with binary surfactant mixtures*. Langmuir : the ACS journal of surfaces and colloids, 2014. **30**(44): p. 13353.
12. Georgieva, G.S., et al., *Synergistic Growth of Giant Wormlike Micelles in Ternary Mixed Surfactant Solutions: Effect of Octanoic Acid*. Langmuir : the ACS journal of surfaces and colloids, 2016. **32**(48): p. 12885.
13. Ruiz, M.O., et al., *Equilibrium Distribution Model of Betaine between Surfactant Micelles and Water: Application to a Micellar-Enhanced Ultrafiltration Process*. Industrial & Engineering Chemistry Research, 2010. **49**(14): p. 6578-6586.
14. Joo, K.-M., et al., *Relationship of ceramide-, and free fatty acid-cholesterol ratios in the stratum corneum with skin barrier function of normal, atopic dermatitis lesional and non-lesional skins*. 2015. p. 71-74.
15. Pham, Q.D., et al., *Chemical penetration enhancers in stratum corneum — Relation between molecular effects and barrier function*. Journal of Controlled Release, 2016. **232**: p. 175-187.
16. Smeden, J., et al., *The importance of free fatty acid chain length for the skin barrier function in atopic eczema patients*. Experimental Dermatology, 2014. **23**(1): p. 45-52.
17. Simpson, E.L., et al., *Emollient enhancement of the skin barrier from birth offers effective atopic dermatitis prevention*. The Journal of Allergy and Clinical Immunology, 2014. **134**(4): p. 818-823.
18. Lemery, E., et al., *Surfactants have multi-fold effects on skin barrier function*. European Journal of Dermatology, 2015. **25**(5): p. 424-435.
19. Telofski, L.S., et al., *The Infant Skin Barrier: Can We Preserve, Protect, and Enhance the Barrier?* Dermatology Research and Practice, 2012. **2012**.
20. Walters, R.M., et al., *Cleansing Formulations That Respect Skin Barrier Integrity*. Dermatology Research and Practice, 2012. **2012**.
21. Renoncourt, A., et al., *Specific Alkali Cation Effects in the Transition from Micelles to Vesicles through Salt Addition*. Langmuir, 2007. **23**(5): p. 2376-2381.
22. Dey, D., et al., *Development of hard water sensor using fluorescence resonance energy transfer*. Sensors & Actuators: B. Chemical, 2013. **184**: p. 268-273.
23. Tokatli, C., et al., *Statistical approaches to evaluate the aquatic ecosystem qualities of a significant mining area: Emet stream basin (Turkey)*. Environmental Earth Sciences, 2014. **71**(5): p. 2185-2197.

24. WHO *Hardness in Drinking-water*. 2011.
25. *LabTech; Hard Water Contamination In Homes Costs Unseen Thousands*. 2015: Atlanta. p. 122.
26. *sodium 2-[2-[2-(tridecyloxy)ethoxy]ethoxy]ethyl sulphate CAS#: 25446-78-0*. 2017; Available from: http://www.chemicalbook.com/ProductChemicalPropertiesCB1885437_EN.htm.
27. Pubchem. *Cocamidopropyl betaine*. 2017; Available from: <https://www.ncbi.nlm.nih.gov/pubmed/>.
28. Lee, J., et al., *Shear free and blotless cryo-TEM imaging: a new method for probing early evolution of nanostructures*. *Langmuir : the ACS journal of surfaces and colloids*, 2012. **28**(9): p. 4043.
29. Mukerjee, P., *Critical micelle concentrations of aqueous surfactant systems*, ed. K.J. Mysels and S. United States. National Bureau of. 1971, Washington, D.C.: Washington : U.S. National Bureau of Standards; for sale by the Supt. of Docs., U.S. Govt. Print. Off.
30. Nagarajan, R., *Molecular Packing Parameter and Surfactant Self-Assembly: The Neglected Role of the Surfactant Tail †*. *Langmuir*, 2002. **18**(1): p. 31-38.
31. Raghavan, S.R., H. Edlund, and E.W. Kaler, *Cloud-Point Phenomena in Wormlike Micellar Systems Containing Cationic Surfactant and Salt*. *Langmuir*, 2002. **18**(4): p. 1056-1064.
32. Lu, H., L. Wang, and Z. Huang, *Unusual pH-responsive fluid based on a simple tertiary amine surfactant: the formation of vesicles and wormlike micelles*. *RSC Adv.*, 2014. **4**(93): p. 51519-51527.
33. Bradbury, R., et al., *Impact of model perfume molecules on the self-assembly of anionic surfactant sodium dodecyl 6-benzene sulfonate*. *Langmuir : the ACS journal of surfaces and colloids*, 2013. **29**(10): p. 3234.
34. Tchakalova, V., et al., *Solubilization and interfacial curvature in microemulsions: II. Surfactant efficiency and PIT*. *Colloids and Surfaces A: Physicochemical and Engineering Aspects*, 2008. **331**(1): p. 40-47.
35. Tchakalova, V., et al., *Solubilization and interfacial curvature in microemulsions: I. Interfacial expansion and co-extraction of oil*. *Colloids and Surfaces A: Physicochemical and Engineering Aspects*, 2008. **331**(1): p. 31-39.

36. Hishida, M., Y. Yamamura, and K. Saito, *Salt effects on lamellar repeat distance depending on head groups of neutrally charged lipids*. Langmuir : the ACS journal of surfaces and colloids, 2014. **30**(35): p. 10583.
37. Strey, R., *Phase behavior and interfacial curvature in water-oil-surfactant systems*. Current Opinion in Colloid & Interface Science, 1996. **1**(3): p. 402-410.
38. Balogh, J., et al., *Effects of oil on the curvature elastic properties of nonionic surfactant films: thermodynamics of balanced microemulsions*. Physical review. E, Statistical, nonlinear, and soft matter physics, 2006. **73**(4 Pt 1): p. 041506.
39. Bergström, L.M., *Model calculations of the spontaneous curvature, mean and Gaussian bending constants for a thermodynamically open surfactant film*. Journal of Colloid And Interface Science, 2006. **293**(1): p. 181-193.
40. Balogh, J. and U. Olsson, *Dependence on Oil Chain-Length of the Curvature Elastic Properties of Nonionic Surfactant Films: Droplet Growth from Spheres to a Bicontinuous Network*. Journal of Dispersion Science and Technology, 2007. **28**(2): p. 223-230.
41. Genç, R., M. Ortiz, and C.K. Sullivan, *Curvature-tuned preparation of nanoliposomes*. Langmuir : the ACS journal of surfaces and colloids, 2009. **25**(21): p. 12604.
42. Bergström, L.M., *Bending elasticity of charged surfactant layers: the effect of layer thickness*. Langmuir : the ACS journal of surfaces and colloids, 2006. **22**(8): p. 3678.
43. Szleifer, I., et al., *Molecular theory of curvature elasticity in surfactant films*. The Journal of Chemical Physics, 1990. **92**(11): p. 6800-6817.
44. Cantor, R.S., *Statistical thermodynamics of curvature elasticity in surfactant monolayer films: A molecular approach*. The Journal of Chemical Physics, 1993. **99**(9): p. 7124-7149.
45. Medronho, B., et al., *Shear-induced transitions between a planar lamellar phase and multilamellar vesicles: continuous versus discontinuous transformation*. Langmuir : the ACS journal of surfaces and colloids, 2008. **24**(13): p. 6480.
46. Genty, M., et al., *Characterization of a complex dispersion of multilamellar vesicles*. Kolloid-Zeitschrift und Zeitschrift für Polymere., 2003. **282**(1): p. 32-40.
47. Courbin, L., et al., *Instability of a lamellar phase under shear flow: formation of multilamellar vesicles*. Physical review letters, 2002. **89**(14): p. 148305.

48. Lu, C.Y.D., *Sizes of multilamellar vesicles in shear*. Physical review letters, 2012. **109**(12): p. 128304.
49. Youssry, M., et al., *Effect of shear on vesicle and lamellar phases of DDAB/lecithin ternary systems*. Journal of Colloid And Interface Science, 2011. **358**(2): p. 506-512.
50. Bagdassarian, C.K., et al., *Curvature defects in lamellar phases of amphiphile-water systems*. The Journal of Chemical Physics, 1991. **94**(4): p. 3030-3041.
51. Chen, Y.L., Z. Xu, and J. Israelachvili, *Structure and interactions of surfactant-covered surfaces in nonaqueous (oil-surfactant-water) media*. Langmuir, 1992. **8**(12): p. 2966-2975.